

Closing the Planning-Learning Loop with Application to Autonomous Driving in a Crowd

Panpan Cai and David Hsu, *Fellow, IEEE*

School of Computing, National University of Singapore, 117417 Singapore

Abstract—Imagine an autonomous robot vehicle driving in dense, possibly unregulated urban traffic. To contend with an uncertain, interactive environment with heterogeneous traffic of cars, motorcycles, buses, . . . , the robot vehicle has to plan in both short and long terms in order to drive effectively and approach human-level performance. Planning explicitly over a long time horizon, however, incurs prohibitive computational cost and is impractical under real-time constraints. To achieve real-time performance for large-scale planning, this work introduces *Learning from Tree Search for Driving* (LeTS-Drive), which integrates planning and learning in a closed loop. LeTS-Drive learns a driving policy from a planner, which is based on sparsely-sampled tree search. The learned policy in turn guides online planning for real-time vehicle control. These two steps are repeated to form a closed loop so that the planner and the learner inform each other and improve in synchrony. The entire system can learn on its own in a self-supervised manner, without human effort on explicit data labeling. We applied LeTS-Drive to autonomous driving in crowded urban environments in simulation. Experimental results show clearly that LeTS-Drive outperforms either planning or learning alone, as well as open-loop integration of planning and learning.

Index Terms—Planning under uncertainty, Robot learning, Autonomous driving

I. INTRODUCTION

As robots move closer to our daily lives in offices, homes, or on the road, a major challenge is tackling complex, highly dynamic, and interactive environments. One example is crowd-driving: an autonomous vehicle drives through crowded roads and unsignalized intersections, with heterogeneous traffic flows of cars, motorcycles, buses, . . . (Fig. 1). The many traffic participants act aggressively to compete for the passageway and avoid collisions, leading to complex interactions and sometimes chaotic traffic. To drive effectively in such an environment, the robot vehicle must perform long-term planning in order to hedge against potential hazards in the future and balance short-term and long-term risks. The primary challenge here is the *scalability* of planning in a high-dimensional state space that captures the many traffic participants nearby and their interactions. The challenge compounds with uncertainties in robot control and sensing, as well as unexpected events in the environment.

One common approach to real-time planning under uncertainty is to perform online look-ahead search. The challenge of long-term planning then depends directly on the search horizon H . With increasing H , the size of the search tree grows exponentially. Further, the model error, if any, accumulates and eventually results in sub-optimal action selection. Naturally, we ask: *can we reap the benefits of long-term planning without a deep search?*



Fig. 1. Crowd-driving. Drive through dense, unregulated, heterogeneous traffic of cars, motorcycles, buses, pedestrians, . . . in complex urban maps.

To tackle this challenge, we propose *Learning from Tree Search for Driving* (LeTS-Drive), which integrates planning and learning in a closed loop. LeTS-Drive learns both *from* and *for* planning: the planner provides the data for learning and, at the same time, benefits from learning for improved online planning performance. It comprises two key ideas:

- plan locally and learn globally
- close the planning-learning loop,

so that both planning and learning improve in synchrony. Concretely, the LeTS-Drive plans locally, through online look-ahead search with a short horizon. It relies on learned global priors—a policy neural network and a value neural network—to approximate long-term values and guide the search. In parallel, the LeTS-Drive learner gathers experiences from the online planner. It uses the data to continuously optimize the priors and feed them back to the planner, thus closing the planning-learning loop. See Fig. 2 for an illustration.

LeTS-Drive is flexible and can take advantage of both self-supervised and reinforcement learning. The self-supervised learner fits the policy network and the value network directly to the planner outputs. It then iteratively updates the policy network, using tree search as the policy improvement operator. The reinforcement learner performs independent policy learning, treating the planner as an off-policy actor to provide high-quality exploration and reward.

LeTS-Drive benefits from both planning and learning. The underlying idea aligns in spirit with AlphaGO-Zero [1], which has beat the human world champion of GO, a perfect-information two-player board game, using learning-guided Monte Carlo Tree Search (MCTS). However, driving in dense traffic poses the new challenges of partial observability, complex dynamics, and a heterogeneous set of interactive agents. The resulting uncertainties are major obstacles to scalability.

To tackle uncertainties, LeTS-Drive builds on top of HyP-DESPOT [2], a parallel algorithm for solving partially observ-

able Markov decision processes (POMDPs). By integrating planning and learning, LeTS-Drive successfully tackles large-scale decision-making under uncertainty with many interactive agents. Further, LeTS-Drive provides theoretical guarantee on the near-optimality of its decision, despite using learned global priors to shorten the planning horizon.

Our experiments examine several variants of LeTS-Drive. We consider open-loop and closed-loop integration of planning and learning, as well as self-supervised and reinforcement learners. We evaluate these variants in a realistic simulator, SUMMIT [3], which simulates dense, unregulated urban traffic at worldwide locations. Given any urban map supported by the OpenStreetMap [4], SUMMIT automatically generates realistic traffic, using GAMMA [5], a recently developed traffic model that has been validated on multiple real-world datasets. Our results show that by integrating planning and learning, LeTS-Drive significantly outperforms either planning or learning alone, achieving sophisticated driving behaviors in crowded, chaotic traffic. Further, closed-loop integration enables significantly faster learning and better asymptotic performance than open-loop integration. After training, LeTS-Drive is capable of generalizing to significantly different environments.

In the following, we start with a short review on integrating planning and learning (Section II). We then give an overview of LeTS-Drive (Section III), followed by details on our POMDP model for autonomous driving in a crowd (Section IV), on learning-guided planning (Section V), and on planning-informed learning (Section VI). We report experimental results in Section VII. Finally, we conclude and point out directions for future research. (Section VIII).

II. BACKGROUND

A. Online POMDP Planning

Planning under uncertainty is critical for robust robot performance in complex, dynamic environments. A key challenge is *partial observability*: true system states are not known accurately and only revealed partially from sensor observations. A principled solution is belief-space planning: maintain a *belief* over possible system states, predict possible future states and observations, and optimize the robot’s control policy in simulated hindsight. This process is formalized as the partially observable Markov decision process (POMDP) [6].

Formally, a POMDP model is represented as a tuple (S, A, Z, T, O, R) , where S represents the state space of the world, A denotes the set of all possible actions, and O represents the observation space. The transition function T characterizes the dynamics of the world. When the robot takes an action a at state s , the world transits to a new state s' with a probability $T(s, a, s') = p(s'|s, a)$. After that, the robot receives an observation z with probability $p(z|s', a) = O(s', a, z)$, and also a real-valued reward $R(s, a)$.

To plan, the robot maintains a belief b , *i.e.*, a probability distribution over possible system states in S . POMDP planning searches for a belief-space policy $\pi: B \rightarrow A$ which prescribes for each belief b an action a that optimizes future values. For infinite horizon POMDPs, the value of a policy π at a belief

b is defined as the expected total discounted reward achieved by executing the policy π from b on-wards:

$$V_\pi(b) = \mathbb{E} \left(\sum_{t=0}^{\infty} \gamma^t R(s_t, \pi(b_t)) \mid b_0 = b \right) \quad (1)$$

Complex tasks are usually solved using online planning: at each time step t , the planner computes an optimal action a^* for the current belief b , executes it immediately, and re-plans for the next time step. Online planning is usually performed as a *belief tree search*. The search starts from the current belief and iteratively constructs a tree consisting of all reachable beliefs in the future. The tree recursively branches with feasible actions and possible observations, until reaching a maximum planning horizon. The desired output is an optimal *policy*, π^* , that maximizes the value at the current belief: $V_{\pi^*}(b) = \max_\pi V_\pi(b)$. The optimal policy is achieved by applying the Bellman’s operator at all belief nodes:

$$V(b) = \max_{a \in A} \left\{ R(b, a) + \gamma \sum_{z \in Z} p(z|b, a) V(b') \right\} \quad (2)$$

where b is a belief node and b' is a child node of b .

Upon finishing the search, the robot executes the optimal action and updates the current belief according to the action a_t taken and the observation z_t received, using the Bayes’ rule:

$$b_t(s') = \eta O(s', a_t, z_t) \sum_{s \in S} T(s, a_t, s') b_{t-1}(s), \quad (3)$$

where η is the normalization constant. The new belief b_t then becomes the entry point of the next planning cycle.

POMDP planning suffers from the well-known “curse of dimensionality” and “curse of history” [6]. State-of-the-art belief tree search algorithms, POMCP [7] and DESPOT [8], have made online POMDP planning practical for real-world tasks such as autonomous driving [9], [10], clutter manipulation [11], multi-agent planning [12], *etc.*. The core ideas are Monte Carlo sampling and heuristic tree search. Specifically, DESPOT samples a fixed set of trajectories, each representing a sequence of state transitions and observations, and then use the sampled trajectories to construct a sparse belief tree. The belief tree search is guided by heuristics, including lower-bound and upper-bound value estimations. The search terminates at any time and outputs a near-optimal action. HyP-DESPOT [2] extends DESPOT through parallelization, which enables real-time performance on large-scale POMDP planning tasks.

B. Integrating Planning and Learning

Recent research seeks to integrate planning and learning to benefit from both the power of explicit reasoning and the robustness of learning from data. One approach is to impose a planning algorithm as the structure prior on the neural network (NN) architecture for learning, so that both the model and algorithm parameters are trained jointly end-to-end [13], [14], [15], [16], [17], [18]. Differentiable algorithms like UPN [17] and DPC [18] have implemented trajectory

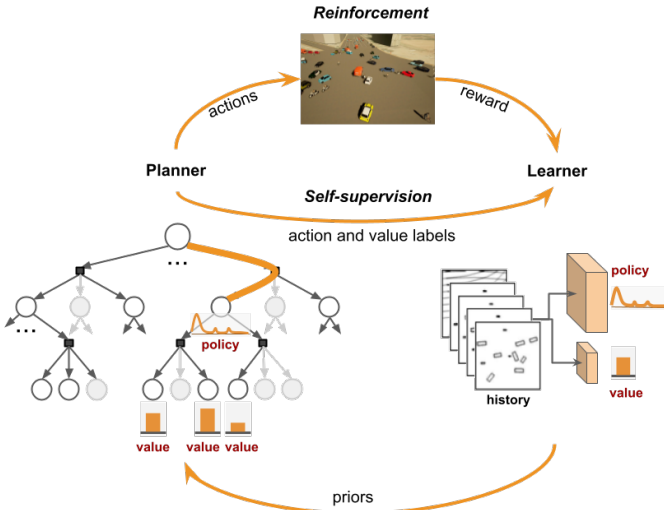


Fig. 2. LeTS-Drive integrates online planning with self-supervised learning or reinforcement learning to close the planning-learning loop.

optimization and model predictive control using neural networks. For MDP/POMDP planning, VIN [13] and QMDP-Net [14] encode the value iteration algorithm in an NN to solve navigation tasks. As expected, the learned networks face the same challenge of scalability as the underlying algorithm: value iteration works well only in low-dimensional discrete state spaces. To address the challenge, TreeQN embeds a fixed forward search tree into an NN [15]. MCTS-Net further enables dynamic tree search by learning differentiable tree search operators [16].

Another approach is to inject learned components into planning. A natural choice is to learn the dynamics and observation models and utilize them for planning or optimal control [19], [20]. One may also learn search heuristics [21], sampling distributions [22], local navigation goals [23], or macro-actions [24], and use them to assist planning. Our earlier work [21] learns policy and value networks as heuristics, and performs planning and learning in two phases. In the offline phase, it learns a policy and the corresponding value function by imitating a standard belief tree search expert. In the online phase, it uses the learned policy and value functions to guide the belief tree search. This algorithm has demonstrated success in driving among a crowd of pedestrians. However, its performance is inherently limited by the quality of the offline expert and the time allowed for online planning.

LeTS-Drive improves our earlier algorithm [21] by closing the planning-learning loop. The new algorithm learns from scratch in a single phase: it improves both planning and learning in synchrony, while collecting more data. The algorithm learns efficiently both from an evolving planner and from environment feedback. While using priors learned approximately, it guarantees the near-optimality of planning.

III. OVERVIEW

LeTS-Drive consists of two interacting components: a planner and a learner (Fig. 2). It starts with randomly initialized policy and value networks. The planner and the learner run

concurrently. Together they form a closed loop between planning and learning.

The planner acts episodically to collect driving data. In each episode, the planner fetches the latest policy and value priors stored in a buffer, shared between the planner and the learner, and uses them to perform belief tree search for real-time driving. Each episode consists of a few minutes of continuous driving and terminates when the vehicle exits the range of the map. Multiple “actors”, *i.e.*, planner instances, execute asynchronously. In simulation, they run in multiple simulator instances. In the real world, they would drive different vehicles. Upon finishing an episode, the planner sends a labeled driving trajectory to the replay buffer shared with the learner. It then proceeds to the next episode.

Concurrently, the learner repeatedly samples data from the replay buffer and uses them to optimize the policy and value priors. In each training iteration, the learner samples a fixed number of data batches and updates the prior networks using gradient descent. For self-supervised learning, it fits the priors to the labelled trajectories of action-value pairs. For reinforcement learning, it reinforces the prior policy using rewards collected by the planner. At the end of the iteration, the learner updates the prior networks in the shared prior buffer and proceeds to the next training iteration.

The planning-learning loop continues until reaching convergence or a maximum time limit. Upon completion, LeTS-Drive provides two policies: a *planner policy* that uses guided belief tree search to drive a vehicle and a *learner policy* that directly maps state histories to driving actions, using the policy network. Both are useful. The learner policy directly maps state histories to actions. It is simple and fast. The planner policy performs anytime belief tree search using the learner policy as the prior. It improves the quality of action in complex situations. If the search tree depth is 0, the planner policy reverts back to the learner policy conceptually.

IV. POMDP FOR DRIVING IN A CROWD

We formulate crowd-driving as a POMDP to plan under the uncertainties in the *intentions* and *attentions* of *exo-agents*. An *exo-agent* is a traffic participant potentially interfering with the *ego-vehicle*. The intention of an *exo-agent* specifies which route on the urban map it intends to take, and its attention specifies whether it will actively avoid collision with others (attentive) or not (distracted). The formulation is similar to the model described in [3] but further optimized for real-time planning and the integration with learning. We have replaced primitive steering actions with lane-keeping/changing decisions. The new action space thus consists of lane decisions and longitudinal accelerations. This action model fully leverages urban roads’ structure and thus reduces the computational complexity of optimal planning. The model also has a factored reward function to facilitate value learning. In this paper, we still refer to the new model as Context-POMDP, to be presented below.

A. States and Observations

A state in Context-POMDP includes both discrete-valued hidden states and continuous-valued observable states:

- Observable state of the ego-vehicle, $s_c = (x, y, \phi, \mu)$, including the position (x, y) , heading direction ϕ , and its intended route μ on the urban map.
- Observable states of exo-agents, $\{s_i = (x, y, \vec{v})\}_{i \in I_{exo}}$, including the position (x, y) and the current velocity \vec{v} of each exo-agent. I_{exo} defines the indices of exo-agents.
- Hidden variables of exo-agents, $\{\theta_i = (t_i, \mu_i)\}_{i \in I_{exo}}$, including the driver’s attention (attentive / distracted) and the intended route of the i th traffic agent.

We assume that the ego-vehicle can observe its own state and coarsely discretized values of the observable states of exo-agents. Hidden variables of exo-agents can only be inferred from history and modeled with distributions.

A *belief* b thus encodes 1) observable states of all agents, and 2) the posterior distribution over exo-agents’ hidden variables (intentions and attentions). The belief is tracked using Bayesian filtering [25] according to the observed interaction history.

B. Actions

An action of the ego-vehicle is a combination of lane-keeping/changing decisions and longitudinal accelerations. Each dimension of the action space contains three possible values: for lane decisions, $\{Left, Keep, Right\}$, and for accelerations, $\{Acc, Maintain, Dec\}$. Lane decisions are executed using a pure-pursuit algorithm [26] to track the center paths of the intended lanes. Acceleration values for *Acc* and *Dec* are 3 m/s^2 and -3 m/s^2 , respectively. The maximum speed of the ego-vehicle is 6 m/s , from which it takes 2 seconds to reach a full stop.

C. State Transitions

The transition model simulates the movements of all agents using their own motion models. In the low-level, kinematics of all vehicle-like agents are simulated using bicycle models [26], while kinematics of pedestrians are treated as holonomic. Behavior-wise, all traffic agents tend to track the center paths of their intended routes. Among them, distracted agents track their intended paths with the observed speeds; Attentive agents additionally use GAMMA [5], an optimal reciprocal collision avoidance model, to interact with surrounding agents, by possibly deviating from the intended paths. Finally, we perturb the displacements of all agents with Gaussian noises to model the stochasticity of human behaviors.

D. Rewards

The reward function is defined as follows. When the vehicle collides with any exo-agent or the road edge, we assign a large penalty, $R_{col} = -1000 \times (v^2 + 0.5)$, increasing with the colliding speed v . For efficiency, we assign each time step a speed penalty $R_v = 4.0(v - v_{max})/v_{max}$ to encourage driving at the maximum speed $v_{max} = 6.0 \text{ m/s}$. We further impose a smoothness penalty $R_{acc} = -0.1$ for each deceleration to penalize excessive speed changes, and a penalty of $R_{change} = -4.0$ for each lane change to avoid jerky paths. The full reward function is the addition of the above components.

E. Factoring Reward and Value Functions

The above reward function effectively encodes the objective of safe, efficient, and smooth driving. However, it leads to a highly non-smooth value function. The magnitude of values would drastically increase near collision events. To facilitate value learning, we have further factored the value function into two smooth factors: a *safe-driving factor* capturing efficiency rewards and smoothness penalties under safe-driving scenarios, and a *collision factor* that captures collision risks and the corresponding penalties. The full value function is a weighted sum of the two smooth factors. See Appendix A for how a factored value function is constructed according to this factored reward function via modified backup in the belief tree search.

V. LEARNING-GUIDED PLANNING

The planner in LeTS-Drive takes as input the current belief over agents’ physical states, intentions, attentions, as well as a map of the urban environment, and outputs real-time, optimal driving actions for the ego-vehicle. In particular, the planner solves the Context-POMDP problem using online belief tree search, and augments its search heuristics using the learned global priors—the policy network and the value network. We also introduce additional techniques to ensure the convergence and near-optimally of planning despite searching with learned heuristics.

The integration of learned priors brings multiple benefits here. From the planning perspective, this largely improves solution qualities under real-time constraints and prevents deep searching trees that cause major problems in long-term planning; From the learning perspective, the belief tree search offers high-quality supervision signals to the learner, serving as a policy improvement operator.

A. Online Belief Tree Search

LeTS-Drive uses HyP-DESPOT [8], a state-of-the-art online belief tree search algorithm, to perform planning. Here, we provide a brief summary of HyP-DESPOT, and refer readers to [2] for further details.

HyP-DESPOT samples a small set of K scenarios as representatives of the stochastic future. Each scenario, $\phi = (s_0, \varphi_1, \varphi_2, \dots)$, contains a sampled initial state s_0 and a sequence of random numbers $\varphi_1, \varphi_2, \dots$ that determinize the outcomes of future actions and observations. HyP-DESPOT constructs a sparse belief tree conditioned on the sampled scenarios. The root node of the tree contains the sampled initial states in all scenarios. The tree then recursively branches with all possible robot actions and the observations encountered under the sampled scenarios. Each node b in the tree thus captures a subset of scenarios Φ_b , whose updated states approximate a future belief.

To compute the optimal policy, the algorithm maintains for each node an *upper bound* and a *lower bound* of the optimal value, u and l , estimated for the corresponding belief. At leaf nodes, HyP-DESPOT uses Monte Carlo (MC) roll-outs to initialize *true* lower bounds and explicit heuristic functions to initialize *true* upper bounds (there generally exist ones that can

be easily written down). These values get constantly updated when searching below a node. We refer to upper and lower bounds calculated in such ways as the *MC value estimations*.

HyP-DESPOT performs anytime heuristic search to construct the belief tree. In each iteration or *trial*, HyP-DESPOT starts from the root node b_0 and searches a single *exploration path* down to a leaf and expands the tree. At each node along the path, HyP-DESPOT heuristically chooses an action branch and an observation branch under it to *explore* according to the upper bound and lower bound values. When reaching a leaf node, HyP-DESPOT *expands* it by simulating the sampled scenarios forward using all possible next actions and creates child nodes according to the sampled observations. Then, it *initializes* for the new nodes the upper bound and lower bound values using MC estimations. The traversal continues until further expansions become no longer beneficial, HyP-DESPOT thus ends the trial and immediately *backs up* new information to the root following the Bellman’s operator and update upper bounds and lower bounds for belief nodes along the way. A new trial is then launched. Multiple trials can happen in parallel to collaboratively expand the tree. The search terminates until the gap between the upper and lower bounds at the root is sufficiently small or the planning time limit is reached.

B. Incorporating Global Priors

Our planner extends HyP-DESPOT by incorporating the learned global priors to guide exploration and initialize leaf nodes. Fig. 2 (left) illustrates the guided search.

The policy network is queried at each *tree node* to provide *prior probabilities* over actions. These probabilities are used to bias action explorations. Specifically, a trial visiting a node b will select a children action branch to explore according to a UCB-like heuristics:

$$a^* = \arg \max_{a \in A} \left\{ u(b, a) + c\pi_\theta(a|x_b) \sqrt{\frac{N(b)}{N(b, a) + 1}} \right\} \quad (4)$$

The first term $u(b, a)$ represents the upper bound value to be achieved if conducting action a at b . The heuristics thus prioritize actions with higher optimistic outcomes. The second term is an exploration bonus. As in HyP-DESPOT, the bonus depends on the visitation count of the node, $N(b)$, and the visitation count of its children action branch, $N(b, a)$. This term thus encourages to explore less-visited actions. In LeTS-Drive, we additionally inject the prior probabilities $\pi_\theta(\cdot|x_b)$ over actions into the bonus, where x_b is the 4-step history at b encoded as images and input to the policy network π_θ . This term assigns higher bonuses to favorable actions suggested by the prior policy. During the first time visiting node b , the upper bound and visitation counts are mostly uninformative. Thus the search policy would be strongly biased towards the prior policy. After sufficient search, the upper bound values will start to take over.

The value network is queried at each *leaf node* to provide a *prior value* that initializes a value estimation for the leaf node:

$$v_0(b) = v_{\theta'}(x_b) \quad (5)$$

Here, $v_{\theta'}(x_b)$ is the value predicted by the value network $v_{\theta'}$ at history state x_b . By learning from past experience, this prior provides accurate value estimations that can otherwise only be acquired by sufficiently searching the corresponding subtree. It thus eliminates the need for searching a deep tree and improves the solution quality under real-time constraints.

Note that we still estimate the Monte Carlo upper and lower bounds for each node. Such *MC bounds* are used to regulate the *learned values* so that theoretical guarantees of the search can be maintained. This will be discussed in the following section.

C. Performance Guarantee

Specifically, we do the following to ensure the convergence of the search and the near-optimality of solutions:

- 1) During the forward search, we use the MC value estimations, instead of the learned values, to compute the heuristics.
- 2) During backup, we update both the MC value estimations and the learned values for each node. When updating a learned value, we keep it clipped within the MC bounds. We refer to this technique as *value-clipping*.
- 3) Upon finishing the search, we use the (backed-up) learned values at the first layer to make the final decision.

Now, we discuss how these mechanisms maintain convergence.

The convergence and optimality of HyP-DESPOT rely on the assumption that the value estimations provide *true* upper and lower bounds over the optimal value. Using such search heuristics, all beliefs reachable under the sampled scenarios and containing useful information will be visited. The gap between the upper and lower bounds at the root will monotonically decrease to zero when expanding more nodes. Upon convergence, HyP-DESPOT can thus report the converged value and the optimal policy at the root.

Note that the MC value estimations satisfy the true-bound assumption; However, the learned values do not—they can not bound the optimal value from either direction and can be arbitrarily wrong in the worst case. Therefore, they should not be directly used in the forward search heuristics. The MC value estimations are used instead.

Despite using the MC estimations, our heuristics are still different from HyP-DESPOT—we have used prior probabilities in Eqn. (4) to bias the action exploration. We claim that this bias does not harm. Convergence remains guaranteed because of the *optimistic trials* launched periodically in HyP-DESPOT. Such optimistic trials perform unbiased explorations (without exploration bonuses) to ensure visiting all useful reachable beliefs in finite time. The MC value estimations thus converge to the optimal value regardless of the biased explorations in other trials [2].

Next, we apply the value clipping technique to ensure that the learned value do not violate the true upper and lower bounds, thus converges to the optimal value together with them. Particularly, a learned value is recorded and backed up only when it lies within the MC bounds:

$$\hat{l}_0(b) = \min(\max(l_0(b), v_{\theta'}(x_b)), u_0(b)) \quad (6)$$

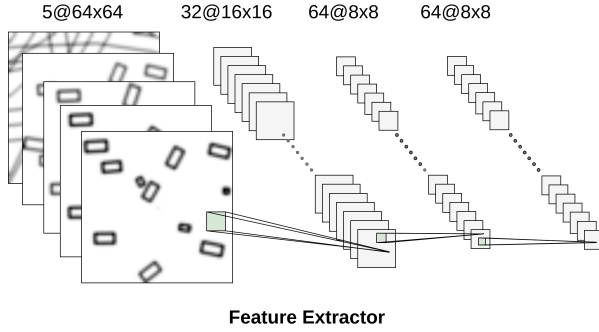


Fig. 3. Neural network architecture of LeTS-Drive.

Once we apply this clipping during leaf node initialization, the same relationship $l(b) \leq \hat{l}(b) \leq u(b)$ will hold for the entire tree, since the Bellman’s back-up operator only contains linear operations and maximization.

With the above, the convergence and near-optimality of the guided search in LeTS-Drive can be guaranteed:

Theorem 1. *Suppose that $\epsilon_0 = u(b_0) - l(b_0)$ is the target gap at the root b_0 to be achieved by the algorithm. The guided belief tree search in LeTS-Drive will converge in finite time. The policy reported by the search is (1) near-optimal when $\epsilon_0 > 0$, and (2) optimal when $\epsilon_0 = 0$ and the regularization constant $\lambda > 0$ (λ is a constant regularizing the size of the search tree [8]).*

Proof. The convergence holds because LeTS-Drive uses the MC estimations during the forward search, thus *exactly the same* heuristics for optimistic trials as HyP-DESPOT. As proven in [2], such optimistic trials always guarantee the convergence of the tree search, regardless of what action exploration mechanism is deployed in other trials. Consequently, the uncertainty gap $u(b_0) - l(b_0)$ at the root node will monotonically decrease and converge to zero.

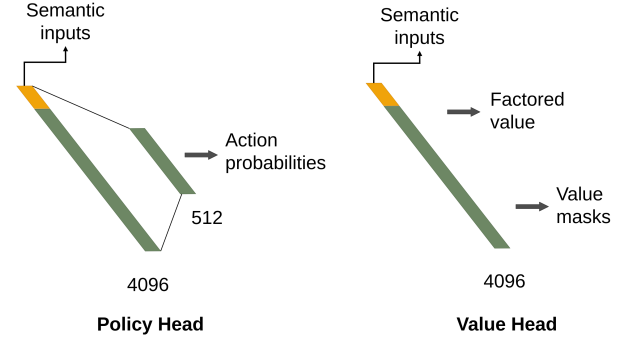
Further, since the learned values are strictly bounded by $[l(b_0), u(b_0)]$, they will also converge to the (near) optimal value upon termination. The corresponding policy reported accordingly is thus also (near) optimal w.r.t the world model used for planning. \square

VI. PLANNING-INFORMED LEARNING

The learner in LeTS-Drive uses the planner’s driving experience to update the prior policy and the prior value. This section will discuss three possible designs of learners—*open-loop self-supervision*, *closed-loop self-supervision*, and *closed-loop reinforcement*. The learners share the same planner counterpart, thus also correspond to three LeTS-Drive variants. In the following, we will first present the prior networks’ architectures, and the form of experience LeTS-Drive learns from, then present the three learner variants’ core ideas and algorithmic details.

A. Prior Networks

The architectures of the policy and value networks are shown in Fig. 3 and described below. Input to the policy and



value networks are top-down rasterized images encoding the history x_b at a belief b . The input consists of 5 channels. Channel 1 – 4 encode the geometry of traffic agents at the current and three past frames; The 5th channel encodes the lane graph of the urban map drawn as a set of poly-lines. All images are registered to the local view of the ego-vehicle for the corresponding time step. They are initially rendered as 1024×1024 images and down-sampled to 64×64 using Gaussian pyramids [27] before inputting to the neural networks.

The policy and value networks use identical feature extractors following the DQN architecture [28]. The input images are processed by three convolutional layers: an input layer with $32 \ 8 \times 8$ kernels with stride 4 and no padding; a middle layer with $64 \ 4 \times 4$ kernels with stride 2 and no padding; and the last layer with $64 \ 3 \times 3$ kernels with stride 1 and no padding. The extractor outputs $64 \ 8 \times 8$ images as hidden features. These features are flattened and concatenated with the semantic inputs, *i.e.*, velocities of the ego-vehicle in the past four frames, and fed to the heads.

Our policy network only has one categorical head to output the distribution over nine possible lane-decision / acceleration combinations. The policy head has two fully-connected (FC) layers mapping from the raw feature vector of length 4096 to an intermediate feature vector of length 512, then to 9 action probabilities. The value network, instead, has two heads corresponding to the factored value function (Appendix A). They include a mask head to output two binary masks for the safe-driving and collision value factors, and a value head to predict the non-zero numbers for the value factors. Both heads have a single FC layer directly mapping the raw features to factored predictions, which are combined to recover the actual value prediction.

B. Representation of Experience

The experience used in LeTS-Drive are driving trajectories collected by real-time planning instances, or *actors*, through driving in the environment. We process such trajectories into a pool of data points, either stored as an offline data set D or a fixed-capacity replay buffer, for offline and online learners, respectively. Each data point is represented as (b, a, b', r, a^*, v^*) , where b is the current belief state, a is the action conducted

by the planner, b' is the updated belief, and r is the step reward received from the environment. Such transition-reward tuples enable reinforcement learning. Additionally, we record two supervision labels: a^* , the optimal action at b reported by the planner, and v^* , the optimal value at b estimated by the planner. These labels enable self-supervised learning.

C. Learners

Now we introduce the learner that uses experiences from the planner to optimize the prior networks. We propose the following learner variants, covering both open-loop and close-loop integration of planning and learning, and leveraging both self-supervised and reinforcement learning:

1) *Open-loop self-supervised learning (Open-SSL)*: In Open-SSL, the integration of planning and learning happens in two phases: offline supervised learning and online guided planning. In the offline phase, Open-SSL learns from a planning expert, supervising the prior networks using standard belief tree search (without priors); In the online phase, it plans with learned priors, using them to guide real-time belief tree search. No further data is fed back to the learner during the online stage. The planner and the learner thus comprise an “open-loop” architecture. This architecture is a modified version of our earlier work [21] extended to perform near-optimal planning for on-road urban driving.

At training time, Open-SSL first collects an offline data set using HyP-DESPOT as the driving expert. Then, the learner fits the policy network to the planner’s actions, and fits the value network to the planner’s value estimations. It uses cross-entropy loss (CEL) for policy predictions and mean-square errors (MSE) for value predictions. To facilitate value learning, we have further decomposed the value loss into safe-driving and collision factors following the factorization of the planner’s value function (Section IV-E). Details are explained in Appendix B1.

At execution time, Open-SSL performs belief tree search to synthesize optimal, real-time driving policies using the learned priors as guidance (as described in Section V). Open-SSL thus benefits from both local planning and global learning. However, the limitation is that it cannot leverage new data generated by the stronger, guided planner.

2) *Closed-loop self-supervised learning (Closed-SSL)*: Closed-SSL improves over Open-SSL by letting the learner receive online experiences from the *guided* planner and constantly feed updated priors back to the planner, to improve the two components in synchrony.

Closed-SSL executes planning and learning in a closed-loop system, as shown in Fig. 2. The system comprises multiple asynchronous planner actors and a learner. During training, actors use the latest priors to plan for driving and collect labeled trajectories from the environment. Such experiences are stored in a fixed-capacity replay buffer. In the meantime, the learner fetches data from the replay buffer and fits the prior networks to the planner-generated labels. It then feeds the new priors back to the planner after a few updates, thus closing the planning-learning loop. The closed-loop system learns from scratch, starting from randomly initialized prior

networks. Training is executed until reaching convergence or a given limit on training time or data.

Closed-SSL is essentially a form of *self-supervised* learning: the planner provides labels to train its own sub-components (the priors). Sample efficiency is achieved by using structured rewards (compiled as values) from the planner as learning signals, instead of unstructured (raw) rewards from the environment.

Closed-SSL can also be viewed as generalized policy iteration [25]: the belief tree search performs policy improvement over the current policy; the learner then updates itself to fit the improved policy. By iterating these two steps, the planner and the learner can together converge to optimal policies defined w.r.t the planner’s world model.

The planning model is, however, an imperfect approximation to the actual environment. Since Closed-SSL entirely relies on the planning model for policy and value computation and thus learning, it can become sensitive to model errors (even though we observe it working well in practice).

3) *Closed-loop reinforcement learning (Closed-RL)*: Closed-RL is thus proposed to hedge against model errors. Closed-RL additionally uses policy gradient [29], [30], [31] to let the prior policy receive and learn from reward feedback from the *actual environment*. By doing so, the prior policy is optimized w.r.t. the true environment dynamics.

Closed-RL shares the same closed-loop architecture and value learner as Closed-SSL. Differently, Closed-RL does not regard planner actors as expert policies, but as *exploration policies*, i.e., exploring driving trajectories and reward signals from the actual environment. Using such data, the learner reinforces the prior policy by estimating its expected value from reward signals along the explored trajectories, and differentiating the value to compute gradients for updating the prior policy (“policy gradient”). Closed-RL thus optimizes the prior policy for its *own* expected value. The prior is thus unaffected by the imperfection of planning models.

Noticeably, the explored driving trajectories are *off-policy*, i.e., not sampled from the distribution induced by the learner policy, but from the distribution induced by the planner. Such trajectories lead to biased value estimations and policy gradients for the learner policy if not properly corrected. Thus, we use an off-policy policy gradient algorithm, soft actor-critic (SAC) [32], to correctly train the prior policy. Details of our SAC implementation are presented in Appendix B2.

VII. EXPERIMENTS

In the experiments, we analyze the following questions:

- 1) Can the integration of planning and learning advance the capability of both?
- 2) What advantages does closed-loop integration bring over open-loop integration?
- 3) How does LeTS-Drive generalize to novel situations and environments?
- 4) What are the benefits of specific algorithmic designs such as value clipping?
- 5) How does the performance of LeTS-Drive scale with the complexity of the scene?

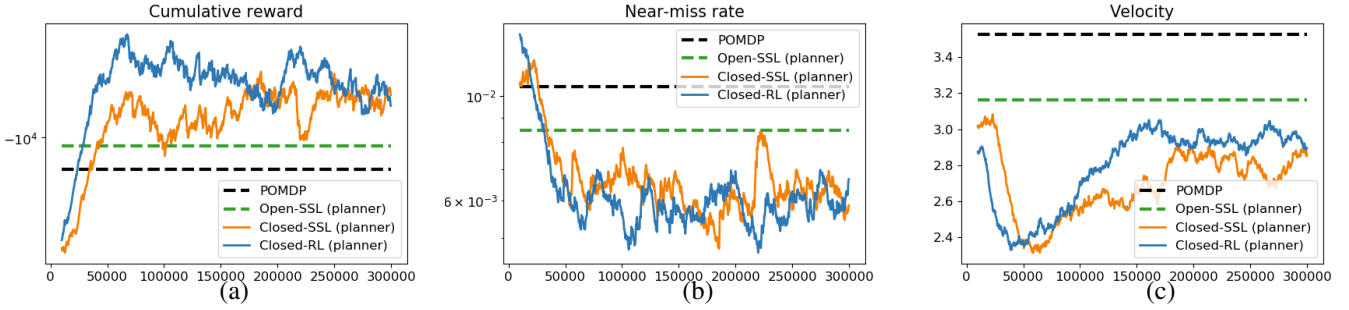


Fig. 4. Learning curves of planner policies in LeTS-Drive compared with POMDP planning. All LeTS-Drive variants achieve significant improvements over POMDP planning. Closed-loop variants, Closed-SSL and Closed-RL, achieve the best sample efficiency and asymptotic performance.

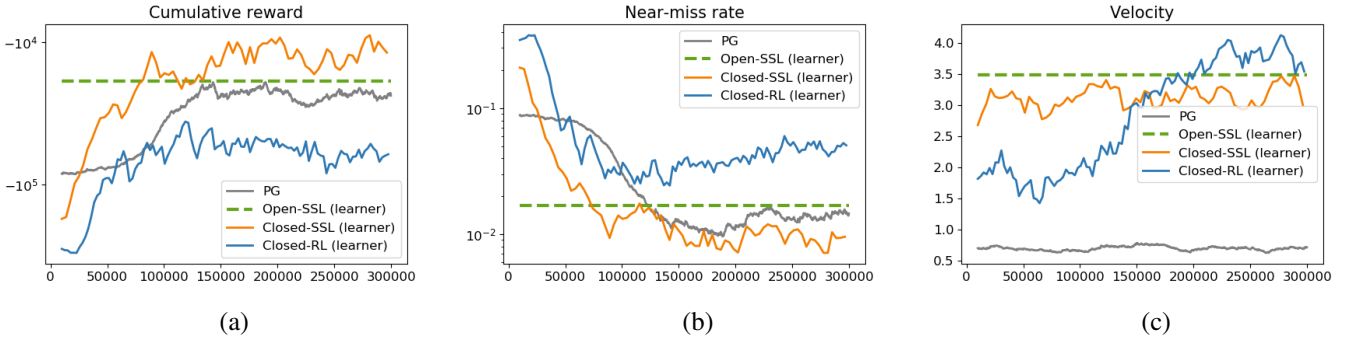


Fig. 5. Learning curves of learner policies in LeTS-Drive, compared with standard policy gradient (PG) and imitation learning (the Open-SSL learner). Self-supervised learning (Closed-SSL) achieves the most effective learner policy among all.

In summary, the integration of planning and learning enables LeTS-Drive to largely advance the capability of both. Closed-loop planning and learning further improves the sample efficiency and asymptotic performance by a large margin. When using self-supervised learning, LeTS-Drive produces the strongest learner policies; when additionally using reinforcement learning, LeTS-Drive achieves the best integrated performance. LeTS-Drive can generalize to unseen random crowds and significantly different maps, and scales up well with the density of the crowd. Value clipping applied in the search not only ensures theoretical guarantees, but also improves the practical performance of LeTS-Drive.

Planner policies of LeTS-Drive are capable of driving successfully and efficiently through dense urban crowds and avoid collision with other agents with sophisticated combinations of accelerations and maneuvers. Example driving clips are provided in the accompanying video or via this link: www.dropbox.com/s/n8t5dxo1i295smy/tro-lets-drive.mp4?dl=0.

A. Experimental Setup

We train and evaluate LeTS-Drive using random crowds at the Meskel-Square intersection (Fig. 1) simulated in SUMMIT [3]. Each instance of urban crowd contains 110 active traffic agents, including trucks, buses, cars, motorcycles, pedestrians, etc.. The intersection is unregulated and all agents drive aggressively, e.g., constantly cutting through the way of and overtaking the ego-vehicle. The ego-vehicle thus needs to account for a large-scale, interactive, and highly dynamic environment.

We tested all three variants of LeTS-Drive, i.e., *Open-SSL*, *Closed-SSL*, *Closed-RL*, and several planning/learning baselines. We use POMDP planning with HyP-DESPT (POMDP) to calibrate the capability of stand-alone planning, and use imitation learning (equivalent to the learner in Open-SSL) and policy gradient (PG) using SAC to calibrate the performance of stand-alone learning. PG is essentially the ablated version of Closed-RL without the help of the planner. The purpose of comparing with PG is not to show generic advancements in reinforcement learning, but the benefits of integrating planning and learning under limited data and short planning time.

In our experiments, all tested planners use 0.3 seconds of planning time and execute at a rate of 3HZ. We train all learning-based algorithms using 3×10^5 data points. Namely, Open-SSL consumes an offline data set of size 3×10^5 and is trained till convergence. Closed-SSL, Closed-RL, and PG use three concurrent actors and a single learner and terminate training after receiving 3×10^5 unique data points, corresponding to approximately 20 hours of training on a single computer using one GTX2080 GPU. The learner in Closed-RL uses the same network architectures as PG. Policy and value networks in all LeTS-Drive variants share the same network architectures.

B. Planner Policies

Fig. 4 shows the learning curves of the *planner policies* in LeTS-Drive. The curves are generated by periodically evaluating the planner policies in SUMMIT throughout training. The curves are averaged over five random seeds for Closed-RL and

three random seeds for Closed-SSL. The main observations are as follows.

The integration of learned priors immediately brings significant performance gain over POMDP planning, even when using the simple open-loop architecture (Open-SSL). The resulting planner policy conducts more cautious driving and leads to fewer near-misses.

By closing the planning-learning loop using self-supervision (Closed-SSL), LeTS-Drive achieves superior sample efficiency, outperforming open-loop integration with around one-tenth of data and achieving much higher asymptotic performance. The resulting planner policy further reduces the near-miss rate by a large margin.

Policy learning using policy gradient (Closed-RL) further improves the integrated performance, as the learner additionally receives feedback from the actual environment. Closed-RL quickly converges to the highest rewards among all during training and delivers the strongest planner policies as Closed-SSL.

We have observed similar learning patterns from Closed-SSL and Closed-RL. Both of them first learn to reduce the near-miss rate by lowering the driving speed. Then, they gradually increase the driving speed with the near-miss rate maintained low. Both training curves have converged after receiving $1.5 \times 10^5 \sim 2 \times 10^5$ data points.

C. Learner Policies

Fig. 5 shows the learning curves of the *learner policies* in LeTS-Drive and other learning-based methods. The curves are generated by periodically evaluating the policy networks in SUMMIT throughout training.

We observe that policy gradient learners (without explicit reasoning) struggle to learn an effective stand-alone policy for crowd-driving given the limited amount of data. This is because the task conveys three distinct local-optima behaviors: non-driving, overly-aggressive driving, and smart collision avoidance (desired). Policy gradient (PG) acquires non-driving behaviors, primarily learning to reduce the near-miss rate, which is safe but inefficient; the learner policy in Closed-RL (using the same policy gradient algorithm as PG) acquires overly-aggressive behaviors, mostly learning to increase the driving velocity, which is efficient but unsafe. Neither of them achieves successful trade-offs between safety and efficiency under the constrained amount of data.

In comparison, self-supervised learning (Closed-SSL) produces smart driving policies with both low near-miss rates and desirable driving efficiency. The final learner policy has matched the performance of POMDP planning, showing the effectiveness of self-supervision in policy learning.

On the other hand, even though Closed-RL fails to learn good stand-alone policies—only coarsely identifies sensible driving behaviors and partially filters bad ones—it has effectively learned useful priors for planning. After the integration, it enables efficient training of the closed-loop system (as shown previously in Fig. 4).

D. Generalization

We now inspect the generalization capability of LeTS-Drive.

TABLE I
GENERALIZATION OVER NEW CROWDS IN THE TRAINING MAP.

| | Reward (10^3) w.r.t. learner | Reward (10^3) w.r.t. POMDP | Near-miss rates | Velocity |
|-------------------------|-------------------------------------|-----------------------------------|--------------------|------------------|
| POMDP | - | 0.00 | 0.0100 | 3.53 ± 0.000 |
| Open-SSL (planner) | +8.34 | +1.54 | 0.0085 | 3.16 ± 0.000 |
| Closed-SSL (planner) | +5.19 | +4.03 | 0.0057 | 2.74 ± 0.003 |
| Closed-RL (planner) | +35.97 | +3.95 | 0.0066 | 3.00 ± 0.005 |

TABLE II
GENERALIZATION OVER NOVEL MAPS.

| | Reward (10^3) w.r.t. POMDP | Near-miss rates | Velocity |
|----------------------|-----------------------------------|-----------------|------------------|
| POMDP | 0.00 | 0.0081 | 3.57 ± 0.026 |
| Open-SSL (planner) | +2.65 | 0.0057 | 3.09 ± 0.000 |
| Closed-SSL (planner) | +3.81 | 0.0049 | 2.74 ± 0.016 |
| Closed-RL (planner) | +4.15 | 0.0052 | 3.03 ± 0.017 |

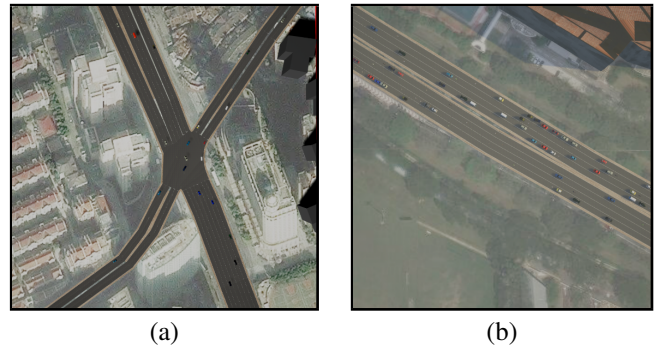


Fig. 6. Novel maps for testing generalization. (a) Shanghai intersection and (b) Singapore highway. Each map is populated with 110 traffic agents in our experiments.

1) *Random test crowds*: Table I shows the results for evaluating the trained planner and learner policies with unseen random crowds on the training map (Meskel intersection). Safety of driving is characterized using the near-miss rate, which represents the portion of time steps when the time to collision is shorter than $0.33s$. The efficiency of driving is measured using the driving speed. The reward w.r.t learner/POMDP shows the improvements of the planner policies over the stand-alone learner policies and POMDP planning on the average cumulative reward. We have calculated each number from more than 1000 test episodes.

The results are generally consistent with those during training, clearly showing the benefits of integrating planning and learning from both directions. All LeTS-Drive planner policies have drastically improved the rewards over POMDP planning and their learning counterparts. Close-loop integration (Closed-SSL and Closed-RL) has achieved significantly higher rewards than the open-loop (Open-SSL), generating planner policies with the lowest near-miss rate and the highest rewards.

We also observe that Closed-SSL equally benefits from planning and learning as shown by similar reward improvements w.r.t. the learner policy and POMDP planning. The improvements in Closed-RL, however, are mostly brought by

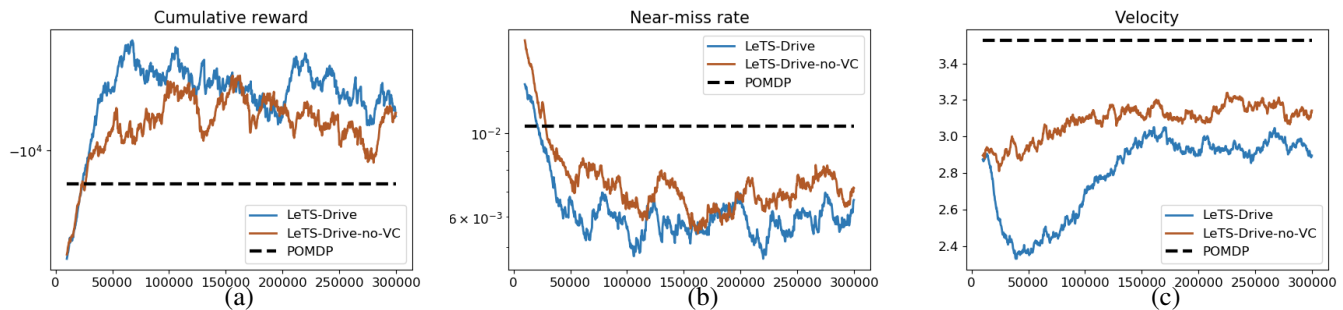


Fig. 7. The effect of value clipping. Compare learning curves of Closed-RL planner policies with and without value clipping.

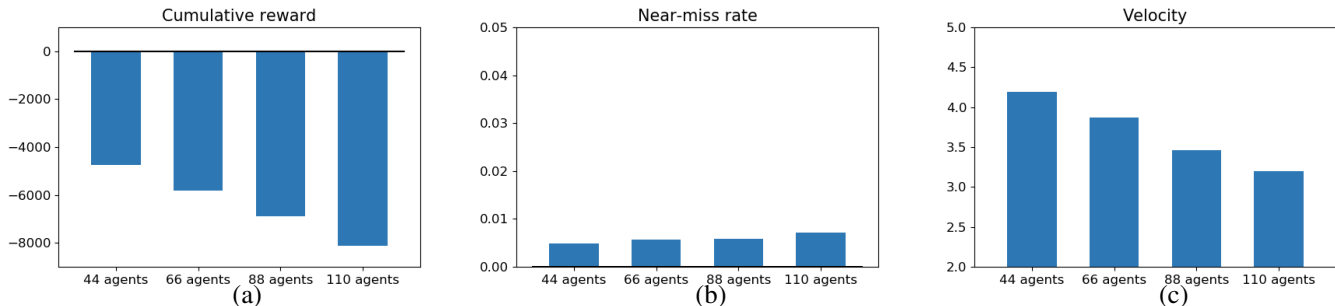


Fig. 8. Scalability with increasing number of agents.

the explicit planning over the learned priors.

2) *Novel test maps*: We further test LeTS-Drive on two significantly different maps: another intersection in Shanghai and a highway in Singapore (Fig. 6). Results are shown in Table II. Despite the extreme setup—training in a single intersection and test on different maps—all variants of LeTS-Drive have successfully generalized to the new environments, largely outperforming POMDP planning. Among them, Closed-SSL and Closed-RL have achieved the best generalized performance. Closed-loop planning and learning brings the same level of benefits as in the training map, delivering the safest planner policies with the highest rewards.

E. The Effect of Value Clipping

Value clipping (Section V-C) is an important algorithmic component that ensures the convergence of the guided belief tree search. We now show its practical effects. Fig. 7 shows the learning curves of LeTS-Drive with and without value clipping. Without value clipping, the planner becomes overly optimistic due to misuse of approximate priors. It seldom attempts to reduce the driving speed during training, thus induces consistently higher near-miss rates. This compromises the rewards throughout training. In contrast, with value clipping, LeTS-Drive becomes more cautious in driving, maintaining significantly lower speeds during the initial course of training. Afterwards, the planner stably improves the driving efficiency and constantly achieves higher rewards. This shows, besides maintaining theoretical guarantees, value clipping also enables more stable and efficient training in practice.

F. Scalability

We have further conducted a scalability test for LeTS-Drive (Closed-RL) by varying the number of agents in the crowd. Fig. 8 shows the test-time performance of LeTS-Drive on the Meskel Square when linearly increasing from 44 agents to 110 agents. Generally, denser crowds compose harder planning problems, increasing the near-miss rates and reducing the planner policy’s driving speed. LeTS-Drive is able to maintain a linear rate of performance decay.

VIII. CONCLUSION AND FUTURE WORK

We have presented a crowd-driving algorithm, LeTS-Drive, which integrates planning and learning by planning locally and learning globally in a closed loop. LeTS-Drive benefits from both self-supervised learning and reinforcement learning. Doing so, LeTS-Drive achieves significant performance gains, compared with planning or learning alone, or open-loop integration of planning and learning. Simulation experiments show that after training, LeTS-Drive drives safely and efficiently through challenging urban traffic intersections with large heterogeneous crowds and generalize to novel environments.

One limitation of LeTS-Drive is potential model errors. Closed-RL alleviates the effect of model errors in policy learning, but not in value learning, which relies on self-supervision. When there are significant model errors, this can lead to inaccurate prior values and compromise the planner’s performance. It is possible to apply reinforcement learning, *e.g.*, temporal difference (TD) learning [33], to learn the values directly, but undesirable because of sample inefficiency. Instead, we can refine value estimates through TD learning after “warming up” through self-supervision.

The current crowd-driving model for LeTS-Drive also requires further improvement on realism, by incorporating comprehensive traffic rules, social norms, and the perception errors on exo-agents' positions, orientations, and velocities. With increased model complexity, we expect LeTS-Drive to provide even more significant performance benefits through integrated planning and learning.

Finally, LeTS-Drive's core idea of integrating planning and learning is not specific to crowd-driving, but applicable in general to many large-scale, long-term planning tasks, such as object manipulation in clutter, multi-agent coordination, *etc.* We will explore these exciting directions as our next step.

REFERENCES

- [1] D. Silver, J. Schrittwieser, K. Simonyan, I. Antonoglou, A. Huang, A. Guez, T. Hubert, L. Baker, M. Lai, A. Bolton, *et al.*, "Mastering the game of go without human knowledge," *Nature*, vol. 550, no. 7676, p. 354, 2017.
- [2] P. Cai, Y. Luo, D. Hsu, and W. S. Lee, "HyP-DESPOT: A hybrid parallel algorithm for online planning under uncertainty," in *Proc. Robotics: Science & Systems*, 2018.
- [3] P. Cai, Y. Lee, Y. Luo, and D. Hsu, "Summit: A simulator for urban driving in massive mixed traffic," *arXiv preprint arXiv:1911.04074*, 2019.
- [4] OpenStreetMap contributors, "Planet dump retrieved from <https://planet.osm.org>." <https://www.openstreetmap.org>, 2017.
- [5] Y. Luo and P. Cai, "Gamma: A general agent motion prediction model for autonomous driving," *arXiv preprint arXiv:1906.01566*, 2019.
- [6] L. P. Kaelbling, M. L. Littman, and A. R. Cassandra, "Planning and acting in partially observable stochastic domains," *Artificial Intelligence*, vol. 101, pp. 99 – 134, 1998.
- [7] D. Silver and J. Veness, "Monte-carlo planning in large POMDPs," in *Advances in Neural Information Processing Systems*.
- [8] N. Ye, A. Somani, D. Hsu, and W. S. Lee, "DESPOT: Online POMDP planning with regularization," *J. Artificial Intelligence Research*, vol. 58, pp. 231–266, 2017.
- [9] H. Bai, S. Cai, N. Ye, D. Hsu, and W. S. Lee, "Intention-aware online POMDP planning for autonomous driving in a crowd," in *Proc. IEEE Int. Conf. on Robotics & Automation*, 2015.
- [10] M. Meghiani, Y. Luo, Q. H. Ho, P. Cai, S. Verma, D. Rus, and D. Hsu, "Context and intention aware planning for urban driving," in *Proc. IEEE/RSJ Int. Conf. on Intelligent Robots & Systems*, 2019.
- [11] Y. Xiao, S. Katt, A. ten Pas, S. Chen, and C. Amato, "Online planning for target object search in clutter under partial observability," in *Proc. IEEE Int. Conf. on Robotics & Automation*, 2019.
- [12] O. Walker, F. Vanegas, and F. Gonzalez, "A framework for multi-agent uav exploration and target-finding in gps-denied and partially observable environments," *Sensors*, vol. 20, no. 17, 2020.
- [13] A. Tamar, Y. Wu, G. Thomas, S. Levine, and P. Abbeel, "Value iteration networks," in *Advances in Neural Information Processing Systems*.
- [14] P. Karkus, D. Hsu, and W. S. Lee, "Qmdp-net: Deep learning for planning under partial observability," in *Advances in Neural Information Processing Systems*.
- [15] G. Farquhar, T. Rocktäschel, M. Igl, and S. Whiteson, "Treeqn and atreec: Differentiable tree-structured models for deep reinforcement learning," *arXiv preprint arXiv:1710.11417*, 2017.
- [16] A. Guez, T. Weber, I. Antonoglou, K. Simonyan, O. Vinyals, D. Wierstra, R. Munos, and D. Silver, "Learning to search with mctsnets," in *Proc. Int. Conf. on Machine Learning*.
- [17] A. Srinivas, A. Jabri, P. Abbeel, S. Levine, and C. Finn, "Universal planning networks: Learning generalizable representations for visuomotor control," in *Proc. Int. Conf. on Machine Learning*.
- [18] J. Dr̄gona, K. Kis, A. Tuor, D. Vr̄abie, and M. Klauco, "Differentiable predictive control: An mpc alternative for unknown nonlinear systems using constrained deep learning," *arXiv preprint arXiv:2011.03699*, 2020.
- [19] D. Hafner, T. Lillicrap, I. Fischer, R. Villegas, D. Ha, H. Lee, and J. Davidson, "Learning latent dynamics for planning from pixels," in *Proc. Int. Conf. on Machine Learning*, 2019.
- [20] K. Fang, Y. Zhu, A. Garg, S. Savarese, and L. Fei-Fei, "Dynamics learning with cascaded variational inference for multi-step manipulation," in *Proc. Conf. on Robot Learning*, 2020.
- [21] P. Cai, Y. Luo, A. Saxena, D. Hsu, and W. S. Lee, "Lets-drive: Driving in a crowd by learning from tree search," in *Proc. Robotics: Science & Systems*, 2019.
- [22] K. Liu, M. Stadler, and N. Roy, "Learned sampling distributions for efficient planning in hybrid geometric and object-level representations," in *Proc. IEEE Int. Conf. on Robotics & Automation*, 2020.
- [23] S. Bansal, V. Tolani, S. Gupta, J. Malik, and C. Tomlin, "Combining optimal control and learning for visual navigation in novel environments," *arXiv preprint arXiv:1903.02531*, 2019.
- [24] Y. Lee, P. Cai, and D. Hsu, "Magic: Learning macro-actions for online pomdp planning using generator-critic," in *Proc. Robotics: Science & Systems*, 2021.
- [25] M. J. Kochenderfer, *Decision Making under Uncertainty: Theory and Application*. MIT press, 2015. Chapter 4, Section 2.3.
- [26] R. Siegwart, I. R. Nourbakhsh, and D. Scaramuzza, *Introduction to autonomous mobile robots*. MIT press, 2011.
- [27] E. H. Adelson, C. H. Anderson, J. R. Bergen, P. J. Burt, and J. M. Ogden, "Pyramid methods in image processing," *RCA engineer*, vol. 29, no. 6, pp. 33–41, 1984.
- [28] V. Mnih, K. Kavukcuoglu, D. Silver, A. A. Rusu, J. Veness, M. G. Bellemare, A. Graves, M. Riedmiller, A. K. Fidjeland, G. Ostrovski, *et al.*, "Human-level control through deep reinforcement learning," *Nature*, vol. 518, no. 7540, pp. 529–533, 2015.
- [29] V. Mnih, A. P. Badia, M. Mirza, A. Graves, T. Lillicrap, T. Harley, D. Silver, and K. Kavukcuoglu, "Asynchronous methods for deep reinforcement learning," in *Proc. Int. Conf. on Machine Learning*.
- [30] T. P. Lillicrap, J. J. Hunt, A. Pritzel, N. Heess, T. Erez, Y. Tassa, D. Silver, and D. Wierstra, "Continuous control with deep reinforcement learning," *arXiv preprint arXiv:1509.02971*, 2015.
- [31] T. Haarnoja, A. Zhou, P. Abbeel, and S. Levine, "Soft actor-critic: Off-policy maximum entropy deep reinforcement learning with a stochastic actor," in *Proc. Int. Conf. on Machine Learning*.
- [32] P. Christodoulou, "Soft actor-critic for discrete action settings," *arXiv preprint arXiv:1910.07207*, 2019.
- [33] R. S. Sutton and A. G. Barto, *Reinforcement learning: An introduction*. MIT press, 2018. Section 11: Off-policy methods with approximation.
- [34] P.-T. De Boer, D. P. Kroese, S. Mannor, and R. Y. Rubinstein, "A tutorial on the cross-entropy method," *Annals of operations research*, vol. 134, no. 1, pp. 19–67, 2005.

APPENDIX

A. Factored reward model

The raw reward function described in Section IV-E is sufficient for planning, but is particularly problematic for value learning due to the existence of rare but critical events, *e.g.*, colliding with others. Particularly, this reward function is smooth at safe belief states, but can change dramatically at proximity to the critical events. To facilitate value learning, we factor our reward function, and consequently the value function, into safe-driving rewards R_s and collision penalties R_c :

$$R = R_s + R_c \quad (7)$$

$$R_s = R_v + R_{acc} + R_{change} \quad (8)$$

$$R_c = R_{col}, \quad (9)$$

where the speed penalty R_v , smoothness penalties R_{acc} and R_{change} , and collision penalty R_{col} are defined as in Section IV-E.

To compute factored values from this reward function, we simply need to record the safe factor V_s and collision factor V_c separately during the backup process in the belief tree search. Particularly, at a belief node b , the Bellman's operator is executed as:

$$a^*(b) = \arg \max_{a \in A} \left\{ R(b, a) + \gamma \sum_{z \in Z} p(z|b, a) V_{MC}(b') \right\} \quad (10)$$

$$V_s(b) = R_s(b, a^*) + \gamma \sum_{z \in Z} p(z|b, a^*) V_s(b') \quad (11)$$

$$V_c(b) = R_c(b, a^*) + \gamma \sum_{z \in Z} p(z|b, a^*) V_c(b') \quad (12)$$

Eqn. (10) denotes the regular value backup process where the best value is chosen according to the MC value estimations V_{MC} . Then the factored values associated with this best action a^* is backed-up to the parent (Eqn. (11-12)).

Factored values at the root node are extracted as supervision labels for the learner. As the two factors are frequently zero, we further decompose the extracted value labels to binary masks and non-zero values before feeding to the learner:

$$V = \mathbb{1}_{|V_s \neq 0} * V_s^- + \mathbb{1}_{|V_c \neq 0} * V_c^-, \quad (13)$$

where V_s^- and V_c^- are non-zero, negative values.

B. Loss functions for learners

1) *Supervision loss*: In self-supervised learners, the policy network π_θ and the value network $v_{\theta'}$ are trained separately using supervised learning using action, mask, and value labels output by the planner. Given a dataset D of size N , the loss functions, $l(\theta, D)$ and $l(\theta', D)$, measure the errors in action and value predictions, respectively:

$$l(\theta, D) = -\frac{1}{N} \sum_i \log \pi_\theta(a^i | x_b^i) - \alpha H(\pi_\theta(\cdot | x_b^i)) \quad (14)$$

$$l(\theta', D) = l_{mask}(\theta', D) + l_{value}(\theta', D) \quad (15)$$

where

$$l_{mask}(\theta', D) = \frac{1}{N} \sum_i (m_s(x_b^i | \theta') - \mathbb{1}_{|V_s^i \neq 0})^2 \quad (16)$$

$$+ (m_c(x_b^i | \theta') - \mathbb{1}_{|V_c^i \neq 0})^2$$

$$l_{value}(\theta', D) = \frac{1}{N} \sum_i (\mathbb{1}_{|V_s^i \neq 0} * v_s(x_b^i | \theta') - V_s^i)^2$$

$$+ (\mathbb{1}_{|V_c^i \neq 0} * v_c(x_b^i | \theta') - V_c^i)^2 \quad (17)$$

Here, x_b^i is the history state in the i th data point; a^i , V_s^i , and V_c^i are the action and value labels obtained from the planner; $m_s(x_b^i | \theta')$ and $m_c(x_b^i | \theta')$ are the mask predictions from the value network; and $v_s(x_b^i | \theta')$ and $v_c(x_b^i | \theta')$ are the value predictions from the value network.

Eqn. (14) represents the cross-entropy loss [34] of the output policy w.r.t. to action labels (the first term) augmented with entropy regularization for the policy itself (the second term). The regularization factor α is tuned online using gradient descent to help maintain a given target entropy of the output policy. This dynamic update rule of α is borrowed from SAC [31]. In our implementation, we set the target entropy to be $0.98 \log |A|$ (targeting at scattered distributions) initially, and gradually anneal it to $0.65 \log |A|$ (targeting at more concentrated distributions). Eqn. (16) defines the prediction loss of the binary masks applied on value factors. Finally, Eqn. (17) defines the regression loss for the non-zero values.

2) *Reinforcement loss*: In the reinforcement learner, we use SAC [31], an off-policy policy-gradient algorithm, to train the policy network. Specifically, we use its discrete-action version presented in [32]. The loss function of the policy learner is:

$$J(\theta) = E_{x_b \sim D} \left[\pi_\theta(x_b)^T [\alpha \log(\pi_\theta(x_b)) - Q_\phi(x_b)] \right] \quad (18)$$

Here, x_b is a sampled history state from the replay buffer; π_θ is the policy network; α is a dynamically-tuned regularization scalar controlling the target entropy of $\pi_\theta(x_b)$; and Q_ϕ is a Q-network trained in a soft-Q learning manner, serving as a differentiable surrogate objective. The Q-network shares the same architecture as the policy network (Fig. 3), but without the softmax applied to the output. Details of the discrete-action SAC can be found in [32].

Note that for policy-gradient, we can not directly apply the reward function described in Section IV-E because of the scale and sparsity of collision penalties. Instead, we use the following smooth reward function in SAC:

$$R = 0.05 \frac{v}{v_{max}} - 0.025 \mathbb{1}_{lane \neq 0} - \frac{1}{9t_c^2} \quad (19)$$

where the first term encourages efficient driving, the second penalizes excessive lane changes, and the third term penalizes proximity to collision events according to the time-to-collision, t_c , estimated using a constant-velocity prediction model.